SCIENCE CHINA Materials ARTICLES

mater.scichina.com link.springer.com

Published online 27 December 2019 | https://doi.org/10.1007/s40843-019-1232-2

Sci China Mater 2020, 63(4): 575–581

Lanthanide near-infrared emission and energy transfer in layered WS_2/MoS_2 heterostructure

Gongxun Bai[1,2], Yongxin Lyu[1], Zehan Wu[1], Shiqing Xu[2*] and Jianhua Hao[1*]

ABSTRACT **Lanthanide ions have attracted great attention due to their distinct photonic properties. The optoelectronic properties and device performance are greatly affected by the interfacial coupling between the layered van der Waals heterostructure, fabricated with two or more transition metal dichalcogenide (TMD) layers. In this work, lanthanide-doped WS_2/MoS_2 layered heterostructures have been constructed through two synthesis steps. The doped thin films are highly textured nanosheets on wafers. Importantly, the as-prepared heterostructure exhibits efficient near-infrared emission in the range of the telecommunication window, owing to energy transfer between lanthanide ions in the two TMD layers. The use of the layered heterostructure allows the decrease of deleterious cross-relaxation due to homogeneous doping or concentration quenching. The energy transfer process was further elaborated in this work. The results suggest that lanthanide ions can effectively extend the emission band of TMD thin films and their heterostructures. The doped TMD heterostructure is highly favourable for constructing atomically thin near-infrared photonic devices.**

Keywords: lanthanide ions, near-infrared luminescence, energy transfer, 2D transition metal dichalcogenide, heterostructure

INTRODUCTION

Recently, a large group of two-dimensional (2D) layered materials, conventionally well-known as the transition metal dichalcongenides (TMDs), such as WS_2 and MoS_2, have been intensified for electronic and optoelectronic applications due to their attractive physical and chemical properties at 2D limit [1–3]. Similar to graphene, layered TMDs possess excellent physcial properties, such as electrical conductivity, thermal stability, flexibility, and mechanical strength [4,5]. In particular, TMD materials possess large exciton binding energies owing to the presence of wide bandgap [6]. Hence, TMD materials have presented considerably potential for next-generation optoelectronic devices and application, including optical sensors, information transmission, solar cells, photodetectors, light-emitting diodes, and display technology [7,8]. Moreover, atomically thin optoelectronic devices can be fabricated by stacking of diverse 2D sublayers into van der Waals (vdW) heterostructures [9–11]. However, the emission of 2D TMDs-based devices are mostly confined in the spectral coverage from red to the near-infrared (NIR) edge. And the tuning of luminescence is mainly governed by excitons, layer numbers, and optical bandgaps. It should be considerably striking in both fundamental study and device applications if the emission bands can be extended to the wide-ranging NIR spectra, especially the telecommunication window. Doping engineering has been demonstrated to be crucial for modulating their intrinsic properties, including band structure, magnetism, chemical sensitivity, semiconductor type. Recently, various doping strategies have been demonstrated to modulate the photoluminscence and electroluminescence in 2D TMDs-based devices [12]. According to previous reports on TMDs, however, the incorporation of transition metal (TM) ions is only capable of adjusting the emitting-wavelength in a relatively narrow spectral range [13,14]. Thus, it is highly desirable to find an effective way to increase the emission bands of 2D TMDs and their vdW heterostructures [1–3].

Lanthanide ions have conventionally been doped into semiconducting or transparent insulating substrates as active centers to emit photons, which cover the ultraviolet (UV), visible, NIR, and mid-infrared (MIR) region [15,16]. Since lanthanide ions have abundant 4f energy states, their emission possess the benefits of high quantum yield, high optical stability, narrow bandwidth, and long lifetime [17,18]. At present, lanthanide-doped optical materials have been broadly applied in many op-

[1] Department of Applied Physics, The Hong Kong Polytechnic University, Hong Kong 999077, China
[2] Institute of Optoelectronic Materials and Devices, China Jiliang University, Hangzhou 310018, China
* Corresponding authors (emails: shiqingxu@cjlu.edu.cn (Xu S); jh.hao@polyu.edu.hk (Hao J))

 © Science China Press and Springer-Verlag GmbH Germany, part of Springer Nature 2019

toelectronic and photonic technologies, including solid-state lighting, telecommunication, biomedicine, etc. [19,20]. For instance, Er^{3+}-doped fiber amplifiers have been practically used in optical fiber communication. Yb^{3+}/Er^{3+}, Yb^{3+}/Tm^{3+} co-doped nanoparticles with up-conversion emission have been applied in biological imaging and therapy [21,22]. Presently, there are only a few reports on the synthesis approach of lanthanide-doped 2D TMDs, including chemical vapor deposition (CVD) and hydrothermal reaction [23]. Specifically, Er^{3+}-doped MoS_2 and Yb^{3+}/Er^{3+} co-doped WSe_2 with NIR emission have been prepared by CVD [24] and pulsed laser deposition [25] in our group. Liu *et al.* [26] have developed Eu^{3+}-doped 2D MoS_2 nanosheets for temperature sensing. Hence, it has been confirmed that lanthanide doping is capable of extending the intrinsic narrow band luminescence of 2D TMD materials. However, the doping concentration is usually limited in a single compound of 2D material, and the emission performance often suffers from deleterious cross relaxation when the lanthanide ions are doped in a homogeneous way [15]. As a research trend, various heterostructures consisting of different 2D compounds are highly desired for constructing atomically thin optoelectronic devices. Inspired by the luminescent core-shell structure which has been extensively studied in earlier reports [27–29], it is anticipated that the doping of lanthanide ions separately in different layers could offer new properties and intriguing characteristics.

In this work, Er^{3+}-doped WS_2 and Yb^{3+}-doped MoS_2 vdW heterostructures have been fabricated for NIR emission. Er^{3+} ions can generate NIR emission around 1540 nm for telecommunication, while Yb^{3+} ions have a great absorption cross-section at 980 nm, which could be used as sensitizers. The crystal structure, chemical compostion, and optical properties have been studied with a serial of techniques. In particular, the energy transfer mechnism between the two TMD vdW heterostructure layers has been investigated.

EXPERIMENTAL SECTION

The lanthanide-doped TMD layered samples were fabricated by magnetron sputtering and CVD. First, the seed layers (Er-doped W) were deposited on SiO_2 (285 nm)/Si substrates by sputtering the metal targets Er and W with different powers. The thickness of seed layer was controlled by varying the deposition time, and the nominal thicknesses are 0.5, 1, 1.5, 2.5 and 5 nm. Subsequently, Er-doped WS_2 nanosheets were prepared by CVD in a horizontal tube furnace. The base pressure of the furnace was pumped down to 50 mTorr, after being flushed with Ar gas. Then the growth pressure was kept at 300 mTorr with 50 sccm Ar flow. The temperature of the thin film was set at 750°C for 20 min. During the reaction, the temperature of the upstream sulphur precursor was held around 200–350°C. To fabricate the lanthanide-doped WS_2/MoS_2 heterostructure, the seed layers (2.5 nm Yb-doped Mo and 2.5 nm Er-doped W) were pre-deposited in sequence. Then the lanthanide-doped heterostructure was obtained after the subsequent sulfurization.

The lanthanide-doped TMD films and heterostructures were characterized by a Raman microscopic Horiba Jobin Yvon HR800 system, under 488 nm laser illumination. The crystal structure was measured by a Rigaku SmartLab X-ray diffractometer. The X-ray photoelectron spectroscopy (XPS) measurements were performed with a SKL-12 multi-technique system. The morphology and chemical compositions were studied by a scanning transmission electron microscope (STEM, JEOL ARM200F) equipped with an energy dispersive X-ray (EDX) spectrometer. The TEM sample was prepared by etching off the silica layer with NaOH and transferring the films on C/Cu TEM grids. The NIR emission spectra were recorded by a spectrophotometer (Edinburgh FLSP920) armed with a 980-nm laser diode.

RESULTS AND DISCUSSION

The optical and electrical properties of thin films strongly depend on the chemical composition and crystal structure. Hence, the phase verification of the as-prepared TMD layers is essential. First, X-ray diffraction (XRD) was studied to identify the crystallographic phase of the as-prepared samples. According to the XRD pattern in Fig. 1a, all the peaks match perfectly with the standard database (JCPDS card No. 08-0237), which can be assigned to the diffraction of hexagonal WS_2. The existence of other impurities, such as Er_2S_3, can be ruled out. The reflection of only intense (00*l*) peak suggests that highly textured WS_2 thin film has been prepared on a SiO_2/Si substrate with favoured alignment of *c*-axis. In general, the texture structure permits the perservation of excellent physical properties of sputtering- and CVD-grown TMDs. Fig. 1b–d show the binding energy profiles of W 4f, S 2p, and Er 4d in the Er-doped and pristine WS_2 nanosheets, respectively. The distinct peaks around 32.38 and 34.55 eV can be assigned to the binding states of W $4f_{7/2}$ and W $4f_{5/2}$ with spin-orbit split separation of 2.17 eV (Fig. 1b). Similarly, two peaks corresponding to the binding states of S $2p_{3/2}$ and S $2p_{1/2}$ are observed at 161.47 and 162.67 eV with a peak separation of 1.2 eV

© Science China Press and Springer-Verlag GmbH Germany, part of Springer Nature 2019

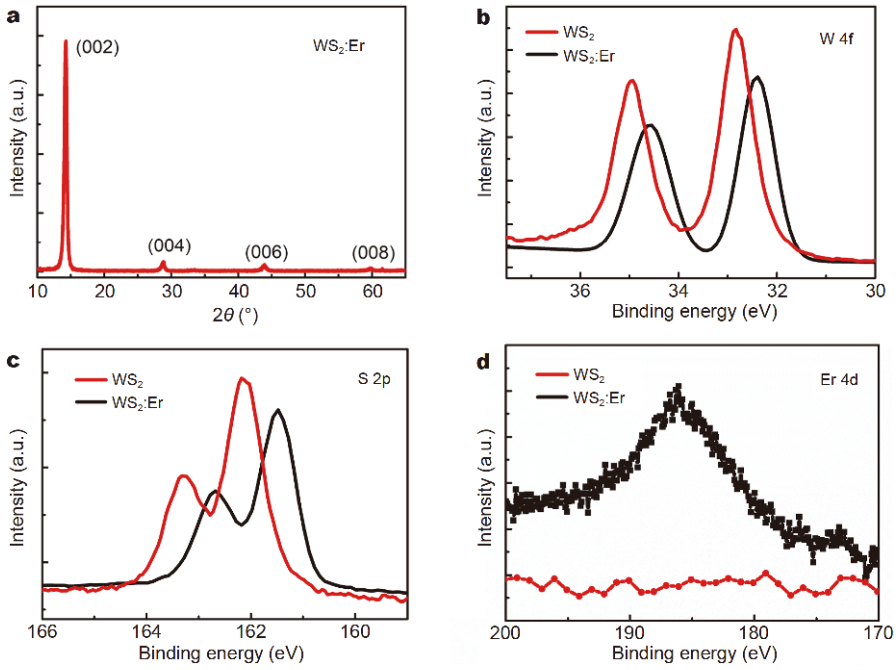

Figure 1 (a) The XRD result of the WS_2:Er thin film. The XPS spectra of the (b) W 4f, (c) S 2p, and (d) Er 4d core levels in the WS_2:Er and WS_2 thin films.

(Fig. 1c). Notably, the core-level peaks of W and S in the WS_2:Er sample show a shift toward lower binding energies compared with the raw WS_2 sample, suggesting a change in the chemical environment. Moreover, the binding energy peak at 185.9 eV can be assinged to the Er 4d core level (Fig. 1d), which is consistent with the previous reports [30]. Both XRD and XPS results suggest the successful implantation of Er ions in WS_2 host matrix while preserving the crystal phase of WS_2.

In the fabricated heterostructure, the WS_2:Er thin film is the active luminescent layer, and the MoS_2:Yb is the sensitized layer. The microstructure of lanthanide-doped MoS_2 thin films has been studied in our previous study [24]. Hence, further investigation on WS_2:Er thin film is the focus of this work. The microstructure and doping profile of the prepared thin films were measured by TEM. Fig. 2a shows the high-resolution TEM image of the fabricated WS_2:Er nanosheets. The hexagonal arrangement of fringes suggests that the WS_2:Er layers are horizontally oriented. The inset electron diffraction pattern displays the polycrystalline structure. Fig. 2b presents the spherical aberration corrected STEM (CS-STEM) image of the WS_2:Er sample. The location of W and Er within the WS_2 lattice can be clearly observed under high angle annular dark field (HAADF) mode. The EDX spectrum in Fig. 2c shows the signals of W, S and Er elements,

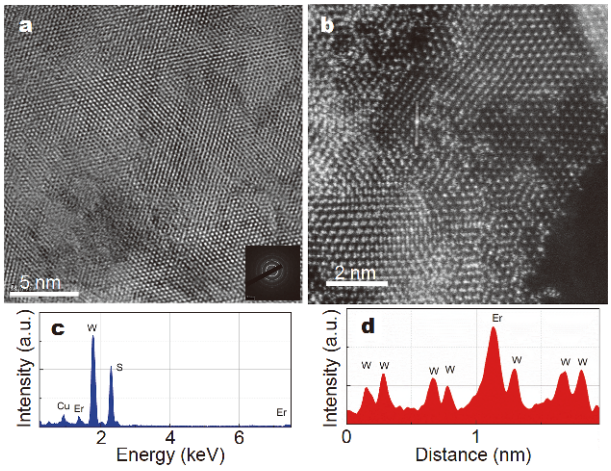

Figure 2 (a) The high-resolution TEM image of the WS_2:Er thin film. (b) The CS-STEM image of the WS_2:Er thin film. (c) The EDX spectrum of the WS_2:Er thin film. (d) The HAADF intensity spectrum of the selected line in (b).

which confirms the incorporation of Er atoms in WS_2 lattice. The measured content of Er^{3+} dopant is 4.5 mol%. The Cu signal originates from the TEM Cu grid. The HAADF intensity in Fig. 2d is generated from the vertical direction of corresponding white line in Fig. 2b. Due to the different atomic radii, the Er atoms show higher in-

 © Science China Press and Springer-Verlag GmbH Germany, part of Springer Nature 2019

tensity compared with W atoms. The intensity spectrum verifies that Er atoms substitute on the site of W atoms in our prepared samples.

The EDX element mapping images are presented in Fig. 3a–d. The distributions of W, S and Er elements are mainly co-localized within the WS_2:Er nanosheets, indicating that the lanthanide Er has been homogeneously doped into WS_2 thin films.

To further study the optical properties of the prepared lanthanide-doped TMD thin films, Raman and photoluminescence spectroscopies have been employed to analyze the thin films with varying layers. The Raman spectra can be used to confirm the characteristic in-plane (E') and out of plane (A'$_1$) vibration modes of the TMD thin films [31]. Here, the resonance Raman spectra of undoped and lanthanide-doped WS_2 thin films were recorded under 488 nm excitation. Fig. 4a displays Raman spectra of the fabricated WS_2:Er thin films with different nominal layer numbers. All the samples present two distinct peaks, which can be attributed to E^1_{2g} and A_{1g} modes, respectively. For the monolayer WS_2 sample, the E^1_{2g} and A_{1g} modes are peaked at 352.1 and 417.3 cm^{-1}, respectively. After doping with lanthanide ions, the resonate transition of monolayer shows very slight shift. With the increase of layer number up to 5, the Raman peak (E^1_{2g} mode) shifts to 352.3 cm^{-1}, and the Raman peak (A_{1g} mode) shifts to 420.1 cm^{-1}. The result suggests that lanthanide-doping shows a small effect on the Raman signature. Fig. 4b presents a comparison among Raman spectra of single-kind WS_2:Er, MoS_2:Yb and their heterostructures. The WS_2:Er layers exhibit Raman peaks at 356.1 and 421.3 cm^{-1}, originating from the E^1_{2g} and A_{1g} modes in WS_2 nanosheets, respectively. The Yb-doped MoS_2 layers present Raman peaks at 384.2 and 408.8 cm^{-1}, corresponding to E^1_{2g} and A_{1g} modes of MoS_2 nanosheets, respectively. This result suggests that we have obtained a WS_2:Er, MoS_2:Yb heterostructure rather than

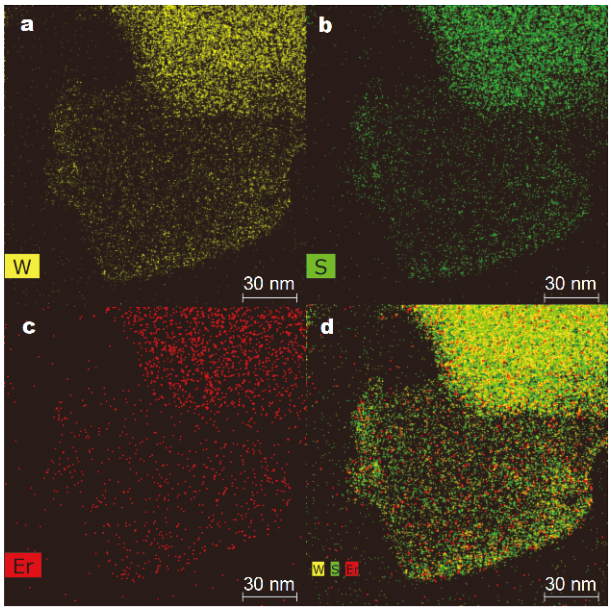

Figure 3 EDX analysis mapping pictures of W, S, and Er elements in the fabricated WS_2:Er thin film.

an alloyed $W_xMo_{1-x}S_2$ thin film, as there would be two main Raman peaks due to the E^1_{2g} and A_{1g} modes in an alloyed $W_xMo_{1-x}S_2$ thin film [32]. The Raman characteristic is similar with the previous result in the WS_2/MoS_2 layered heterostructure [33]. The peak spacing between the E' and A'$_1$ modes recorded from the individual WS_2:Er and MoS_2:Yb thin films are 65.2 and 24.6 cm^{-1}, respectively, suggesting the formation of ~5 layers in each TMD thin films.

Fig. 5a shows the photoluminescence spectra of the prepared WS_2:Er thin films with different nominal layers under 488 nm excitation at room temperature. When increasing the layer number, the peaks of emitting-wavelength exhibit progressive shift to lower energy from 620 to 710 nm. Besides, monolayer WS_2 shows the most

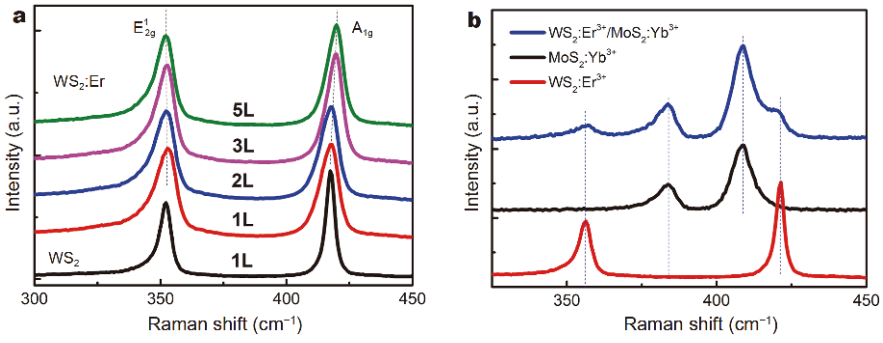

Figure 4 Raman spectra of the fabricated WS_2, WS_2:Er (a), MoS_2:Yb, and TMD heterostructure thin films (b).

© Science China Press and Springer-Verlag GmbH Germany, part of Springer Nature 2019

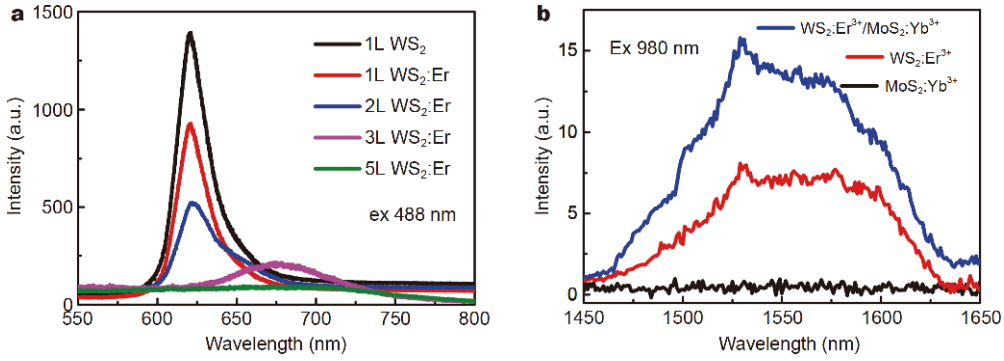

Figure 5 (a) The emission spectra of the fabricated WS_2 thin films with different nominal layers under 488 nm excitation. (b) The NIR emission spectra of the WS_2:Er, MoS_2:Yb, and TMD heterostructure thin films under 980 nm excitation.

intensive emission peak due to the presence of direct bandgap. Under laser excitation at 980 nm, the undoped WS_2 thin film only shows red emission, while both WS_2:Er thin film and WS_2:Er/MoS_2:Yb heterostructure show down-shifting emission around 1550 nm (Fig. 5b). This NIR emission can be attributed to the radiative transition of lanthanide Er^{3+}: $^4I_{13/2} \rightarrow {}^4I_{15/2}$. Compared with the WS_2:Er thin film, the WS_2:Er/MoS_2:Yb heterostructure presents more intensive NIR emission around 1550 nm, and the emission intensity is effectively improved by ~200%. It is deduced that the enhanced NIR emission can be attributed to the energy transfer and the improved absorption section at 980 nm owing to the introduction of MoS_2:Yb heterostructure. It is well acknowledged that the low loss window at 1550 nm is of vital importance in NIR photonics. The ultimate objective of fabricating atomically thin optoelectronic devices has prompted the intensive exploration on 2D TMDs and their heterostructures. Our experimental results in Fig. 5b suggest that the lanthanide-doped heterostructure is capable of extending the intrinsic emission of their TMD host more efficiently compared with single-kind thin films. This finding not only brings profound value to fundamental investigations, but also offers a novel opportunity to the advancement of atomically thin optoelectronic devices in NIR spectra. Fig. 6 shows the schematic of the WS_2:Er/MoS_2:Yb heterostructure. The corresponding energy level scheme and energy transfer mechanism of the proposed lanthanide-doped heterostructure are depicted. Under 980 nm laser pumping, the electrons of Er^{3+} ions at $^4I_{15/2}$ state are populated to $^4I_{11/2}$ state *via* ground state absorption (GSA) in WS_2:Er sublayer. Meanwhile, the electrons of Yb^{3+} ions at $^2F_{7/2}$ state are populated to the $^2F_{5/2}$ state *via* GSA in MoS_2:Yb sublayer. As the absorption section of the Yb^{3+}:$^2F_{5/2}$ state

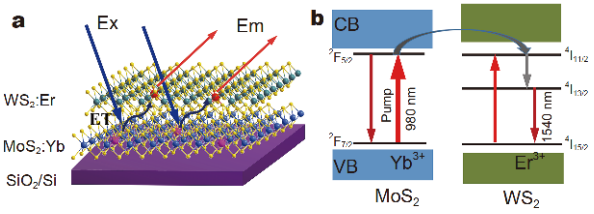

Figure 6 (a) The prepared lanthanide-doped WS_2/MoS_2 heterostructure diagram. (b) The proposed energy transfer mechanism. CB is short for conduction band, VB is short for valence band.

is much larger than that of the Er^{3+}:$^4I_{15/2}$ state, energy transfer occurs from the populated Yb^{3+}:$^2F_{5/2}$ state to the Er^{3+}:$^4I_{11/2}$ state [25,30]. Subsequently, the electrons at the Er^{3+}:$^4I_{11/2}$ state relax to the excited Er^{3+}:$^4I_{13/2}$ state in either radiative or non-radiative way. Finally, the electrons in the Er^{3+}:$^4I_{13/2}$ state radioactively relax to the ground state Er^{3+}:$^4I_{15/2}$, and NIR emission with the wavelength of 1550 nm occurs. Hence, the enhanced NIR emission is generated in the WS_2:Er/MoS_2:Yb heterostructure owing to the lanthanide doping and energy transfer mechanism.

CONCLUSIONS

In conclusion, we have designed and fabricated lanthanide-doped TMD thin films and stacked heterostructure through magnetron sputtering and CVD methods. Comprehensive structural and chemical characterizations suggest that the prepared lanthanide Er^{3+}-doped WS_2 thin film is highly textured nanosheets, and lanthanide ions could be introduced into the TMD lattice. Importantly, the emission of TMD materials can be extended to the telecommunication range under 980 nm excitation. In particular, the lanthanide-doped TMD heterostructure produces efficient NIR emission as a result of energy transfer between WS_2:Er and MoS_2:Yb layers. The lan-

 © Science China Press and Springer-Verlag GmbH Germany, part of Springer Nature 2019

thanide-doped TMD heterostructure is promising for the application in atomically thin NIR optoelectronic and photonic devices.

Received 24 October 2019; accepted 6 December 2019; published online 27 December 2019

1 Liu Y, Weiss NO, Duan X, *et al.* van der Waals heterostructures and devices. Nat Rev Mater, 2016, 1: 16042
2 Desai SB, Madhvapathy SR, Sachid AB, *et al.* MoS_2 transistors with 1-nanometer gate lengths. Science, 2016, 354: 99–102
3 Xu W, Liu W, Schmidt JF, *et al.* Correlated fluorescence blinking in two-dimensional semiconductor heterostructures. Nature, 2016, 541: 62–67
4 Yang Z, Wu Z, Lyu Y, *et al.* Centimeter-scale growth of two-dimensional layered high-mobility bismuth films by pulsed laser deposition. InfoMat, 2019, 1: 98–107
5 Yang Z, Hao J. Progress in pulsed laser deposited two-dimensional layered materials for device applications. J Mater Chem C, 2016, 4: 8859–8878
6 Tan C, Cao X, Wu XJ, *et al.* Recent advances in ultrathin two-dimensional nanomaterials. Chem Rev, 2017, 117: 6225–6331
7 Withers F, Del Pozo-Zamudio O, Mishchenko A, *et al.* Light-emitting diodes by band-structure engineering in van der Waals heterostructures. Nat Mater, 2015, 14: 301–306
8 Wu S, Buckley S, Schaibley JR, *et al.* Monolayer semiconductor nanocavity lasers with ultralow thresholds. Nature, 2015, 520: 69–72
9 Jie W, Yang Z, Bai G, *et al.* Luminescence in 2D materials and van der Waals heterostructures. Adv Opt Mater, 2018, 6: 1701296
10 Chhowalla M, Jena D, Zhang H. Two-dimensional semiconductors for transistors. Nat Rev Mater, 2016, 1: 16052
11 Li Z, Zheng J, Zhang Y, *et al.* Synthesis of ultrathin composition graded doped lateral WSe_2/WS_2 heterostructures. ACS Appl Mater Interfaces, 2017, 9: 34204–34212
12 Suh J, Park TE, Lin DY, *et al.* Doping against the native propensity of MoS_2: Degenerate hole doping by cation substitution. Nano Lett, 2014, 14: 6976–6982
13 Sun QC, Yadgarov L, Rosentsveig R, *et al.* Observation of a Burstein–Moss shift in rhenium-doped MoS_2 nanoparticles. ACS Nano, 2013, 7: 3506–3511
14 Gao J, Kim YD, Liang L, *et al.* Transition-metal substitution doping in synthetic atomically thin semiconductors. Adv Mater, 2016, 28: 9735–9743
15 Yu S, Tu D, Lian W, *et al.* Lanthanide-doped near-infrared II luminescent nanoprobes for bioapplications. Sci China Mater, 2019, 62: 1071–1086
16 Zhang Y, Hao J. Metal-ion doped luminescent thin films for optoelectronic applications. J Mater Chem C, 2013, 1: 5607–5618
17 Huang P, Zheng W, Tu D, *et al.* Unraveling the electronic structures of neodymium in $LiLuF_4$ nanocrystals for ratiometric temperature sensing. Adv Sci, 2019, 6: 1802282
18 Wang Y, Zhou J, Gao J, *et al.* Physical manipulation of lanthanide-activated photoluminescence. Annalen der Physik, 2019, 531: 1900026
19 Deng R, Qin F, Chen R, *et al.* Temporal full-colour tuning through non-steady-state upconversion. Nat Nanotech, 2015, 10: 237–242
20 Bai G, Tsang MK, Hao J. Luminescent ions in advanced composite materials for multifunctional applications. Adv Funct Mater, 2016, 26: 6330–6350
21 Wu X, Zhang Y, Takle K, *et al.* Dye-sensitized core/active shell upconversion nanoparticles for optogenetics and bioimaging applications. ACS Nano, 2016, 10: 1060–1066
22 Dong H, Sun LD, Yan CH. Energy transfer in lanthanide upconversion studies for extended optical applications. Chem Soc Rev, 2015, 44: 1608–1634
23 Cheng L, Yuan C, Shen S, *et al.* Bottom-up synthesis of metal-ion-doped WS_2 nanoflakes for cancer theranostics. ACS Nano, 2015, 9: 11090–11101
24 Bai G, Yuan S, Zhao Y, *et al.* 2D layered materials of rare-earth Er-doped MoS_2 with NIR-to-NIR down- and up-conversion photoluminescence. Adv Mater, 2016, 28: 7472–7477
25 Bai G, Yang Z, Lin H, *et al.* Lanthanide Yb/Er co-doped semiconductor layered WSe_2 nanosheets with near-infrared luminescence at telecommunication wavelengths. Nanoscale, 2018, 10: 9261–9267
26 Liu J, Van Deun R, Kaczmarek AM. Optical thermometry of MoS_2: Eu^{3+} 2D luminescent nanosheets. J Mater Chem C, 2016, 4: 9937–9941
27 Zhou B, Tao L, Chai Y, *et al.* Constructing interfacial energy transfer for photon up- and down-conversion from lanthanides in a core-shell nanostructure. Angew Chem Int Ed, 2016, 128: 1–6
28 Zhou J, Liu Q, Feng W, *et al.* Upconversion luminescent materials: advances and applications. Chem Rev, 2015, 115: 395–465
29 Zhou B, Shi B, Jin D, *et al.* Controlling upconversion nanocrystals for emerging applications. Nat Nanotech, 2015, 10: 924–936
30 Ding M, Chen D, Yin S, *et al.* Simultaneous morphology manipulation and upconversion luminescence enhancement of β-$NaYF_4$: Yb^{3+}/Er^{3+} microcrystals by simply tuning the KF dosage. Sci Rep, 2015, 5: 12745
31 Liu B, Zhao W, Ding Z, *et al.* Engineering bandgaps of monolayer MoS_2 and WS_2 on fluoropolymer substrates by electrostatically tuned many-body effects. Adv Mater, 2016, 28: 6457–6464
32 Sigiro M. Raman scattering characterization of $Mo_xW_{1-x}S_2$ layered mixed crystals. Acta Phys Pol A, 2017, 131: 259–262
33 Tongay S, Fan W, Kang J, *et al.* Tuning interlayer coupling in large-area heterostructures with CVD-grown MoS_2 and WS_2 monolayers. Nano Lett, 2014, 14: 3185–3190

Acknowledgements The authors acknowledge grants from the National Natural Science Foundation of China (61705214) and the Research Grants Council-General Research Fund of Hong Kong (RGC GRF PolyU 153281/16P).

Author contributions The experiments were done by Bai G, Lyu Y, and Wu Z under the instruction of Xu S and Hao J. The manuscript was mainly written by Bai G and Hao J with contributions of all authors. All authors have given approval to the final version of the manuscript.

Conflict of interest The authors declare that they have no conflict of interest.

 © Science China Press and Springer-Verlag GmbH Germany, part of Springer Nature 2019

Gongxun Bai obtained his BSc degree from Huazhong University of Science and Technology, MSc degree from Shanghai Institute of Optics and Fine Mechanics, Chinese Academy of Sciences and PhD degree from the Hong Kong Polytechnic University. Now he is a professor at the Institute of Optoelectronic Materials and Devices, China Jiliang University. His research focuses on low-dimensional optoelectronic materials and devices.

Shiqing Xu received his PhD degree from Shanghai Institute of Optics and Fine Mechanics, Chinese Academy of Sciences. He is currently a professor at the Institute of Optoelectronic Materials and Devices, China Jiliang University. His research interest involves rare earth ions doped functional glasses, optical fibres and luminescent materials for lighting and sensing applications.

Jianhua Hao obtained his BSc, MSc and PhD at Huazhong University of Science and Technology, China. After working at Pennsylvania State University, USA, University of Guelph, Canada and the University of Hong Kong, he joined the Department of Applied Physics in the Hong Kong Polytechnic University as a faculty member in 2006. His research interests include luminescent materials for photonic and biological applications, thin-films and heterostructures, and nanomaterials.

二维层状WS_2/MoS_2异质结中镧系近红外光子发射与能量转移

白功勋[1,2], 吕永昕[1], 吴泽涵[1], 徐时清[2*], 郝建华[1*]

摘要 镧系离子由于其独特的光子特性而备受关注. 二维层状范德华异质结的光电特性和器件性能受到界面耦合的极大影响, 该异质结通常是由两层或多层过渡金属二硫化物(TMD)堆叠而成. 本文通过两步合成构建了镧系离子掺杂的层状WS_2/MoS_2异质结. 所制备的掺杂薄膜是在晶圆衬底上生长的高度织构纳米片. 更重要的是, 由于两个TMD层中镧系离子之间的能量转移, 层状异质结的结构减少了因均匀掺杂或浓度猝灭而引起的无益交叉松弛, 所制备的堆叠异质结能够在近红外通讯窗口产生高效的光子发射. 镧系掺杂和能量转移的研究结果表明, 镧系离子可以有效地扩展TMD薄膜的发射波段及其异质结构. 本工作所发展的镧系掺杂TMD异质结有助于进一步研究原子级超薄近红外光子器件.

 © Science China Press and Springer-Verlag GmbH Germany, part of Springer Nature 2019